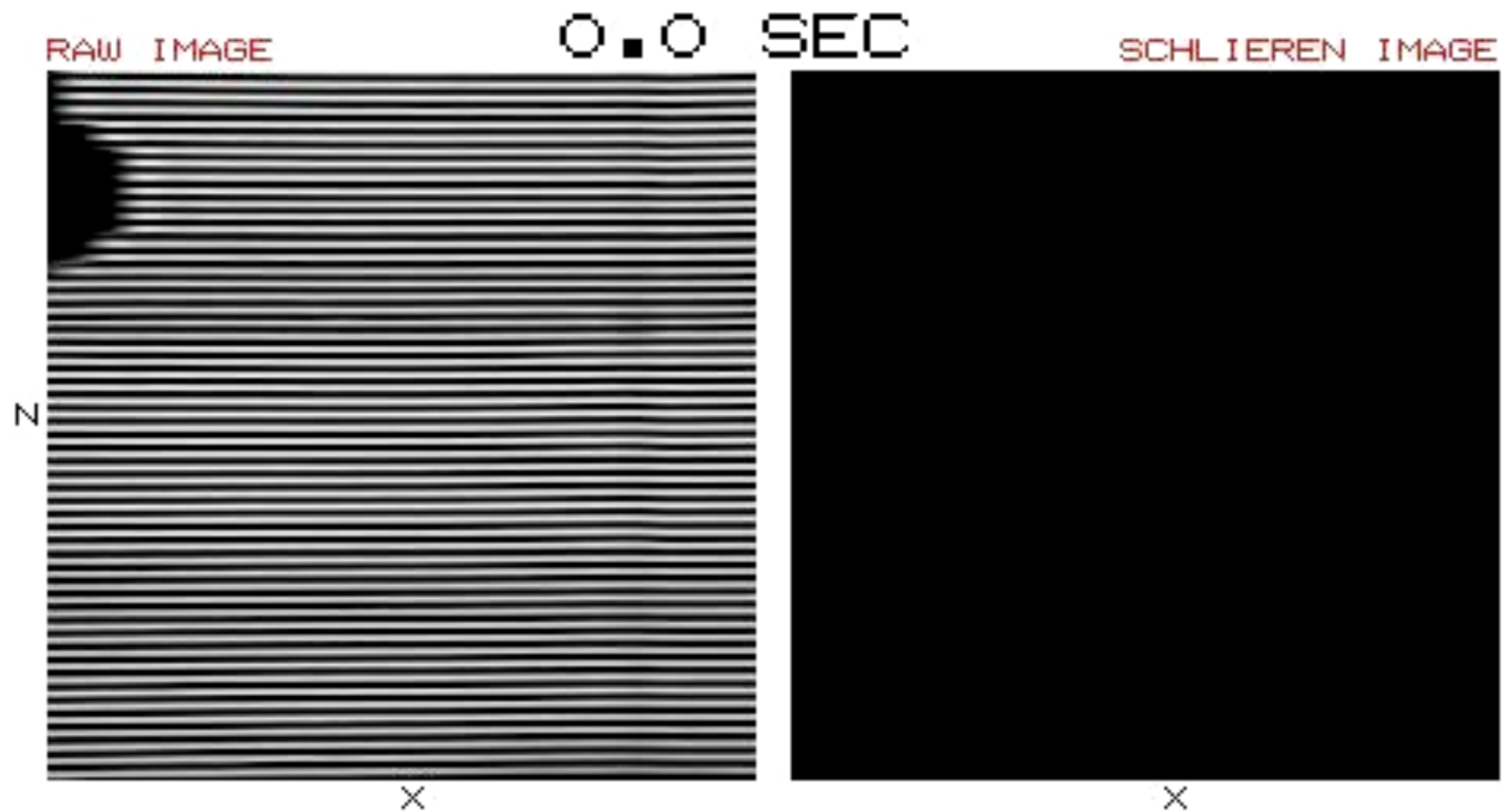


St Andrew's Cross



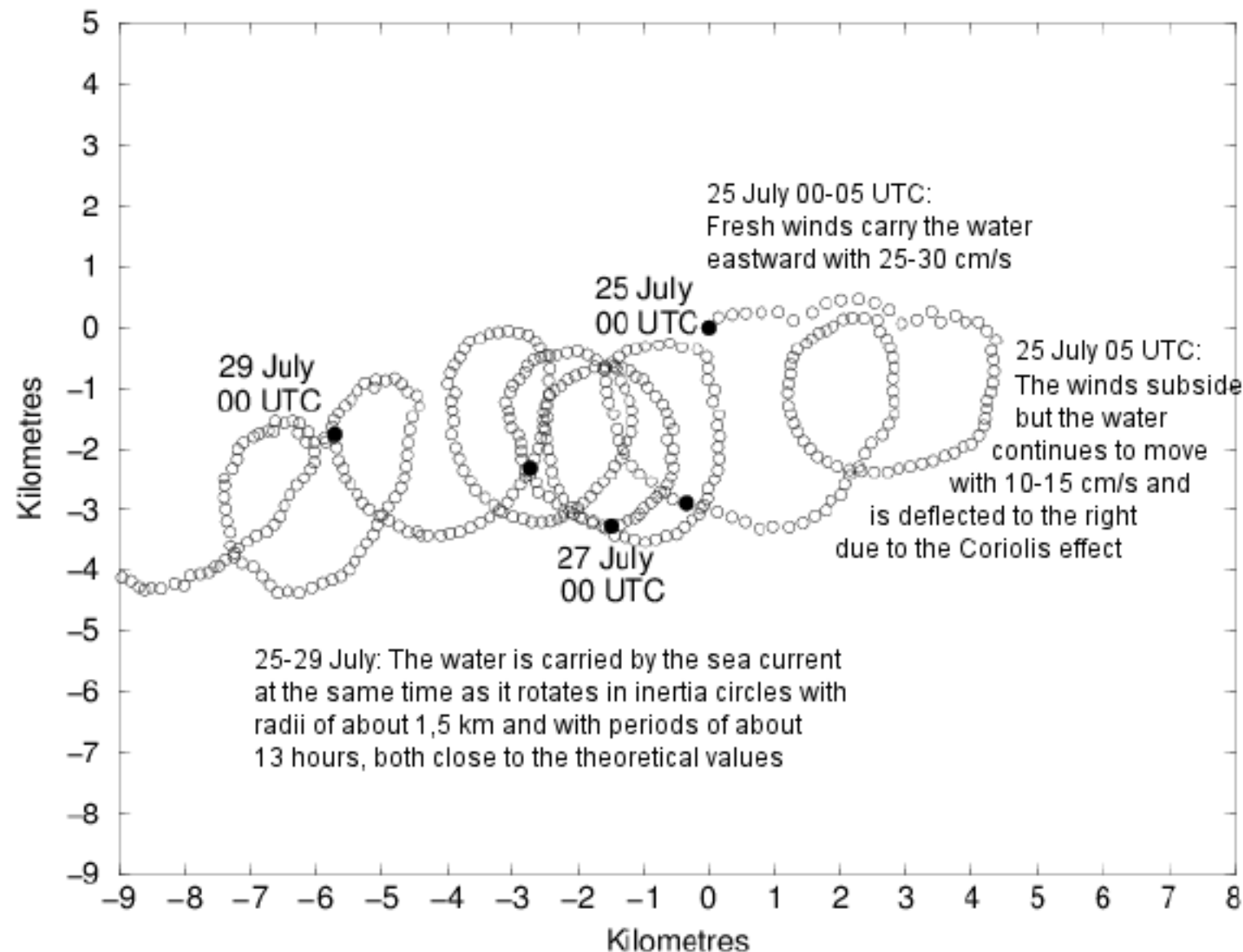
Simulation of Internal Wave Excitation from Oscillatory Forced Patch (Sutherland)

St Andrew's Cross



Laboratory Experiment (Sutherland, 2003)

Inertial oscillations



A drifting buoy set in motion by strong westerly winds in the Baltic Sea in July 1969. When the wind has decreased the uppermost water layers of the oceans tend to follow approximately inertia circles due to the Coriolis effect. This is reflected in the motions of drifting buoys. In the case there are steady ocean currents the trajectories will become cycloides.

Rotary spectra

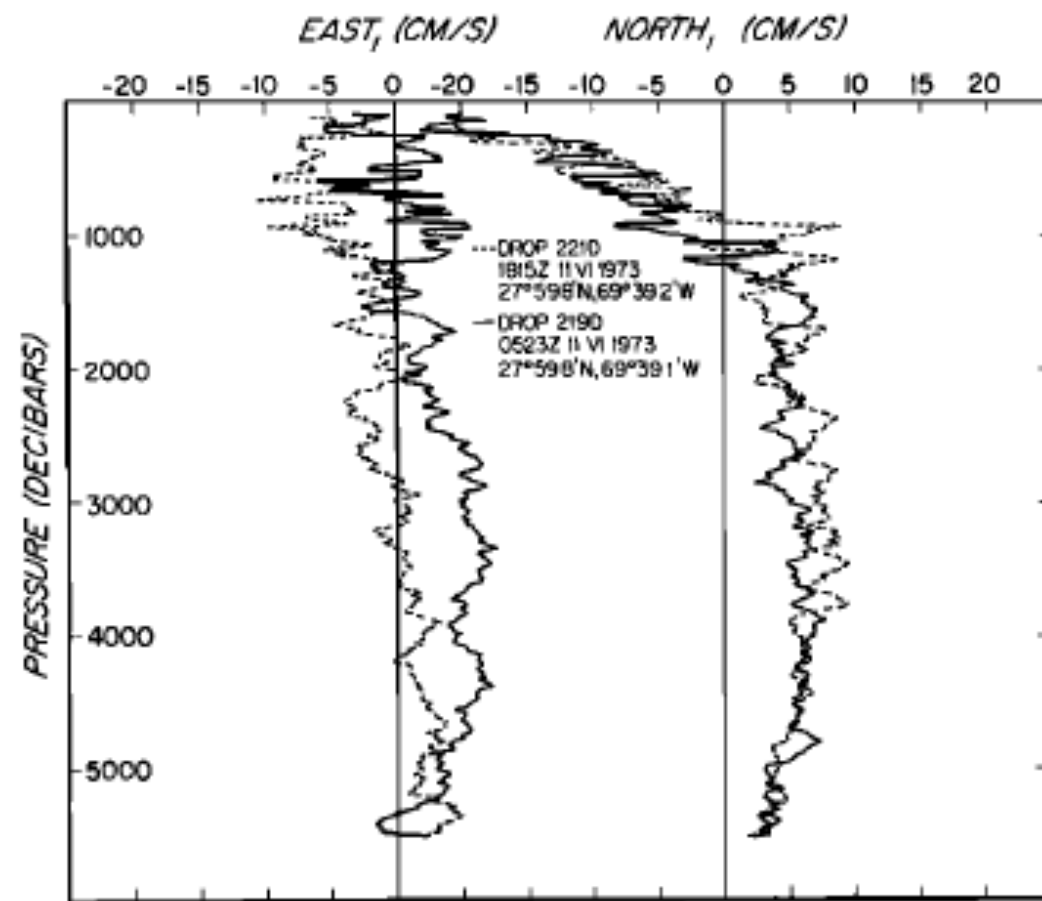


Fig. 1. East and north velocity components for profiles 219D and 221D, taken $\frac{1}{2}$ an inertial period apart.

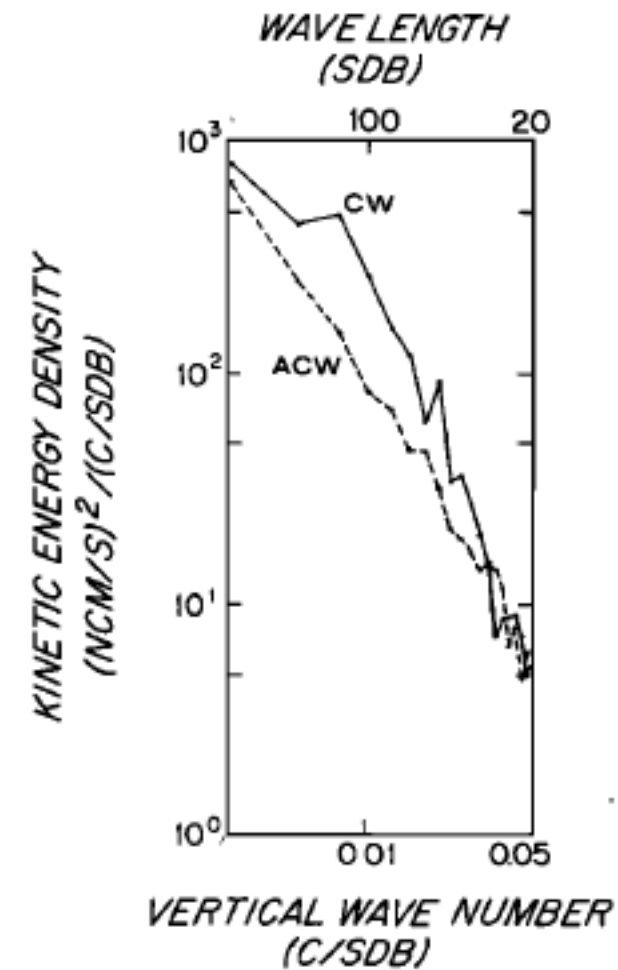
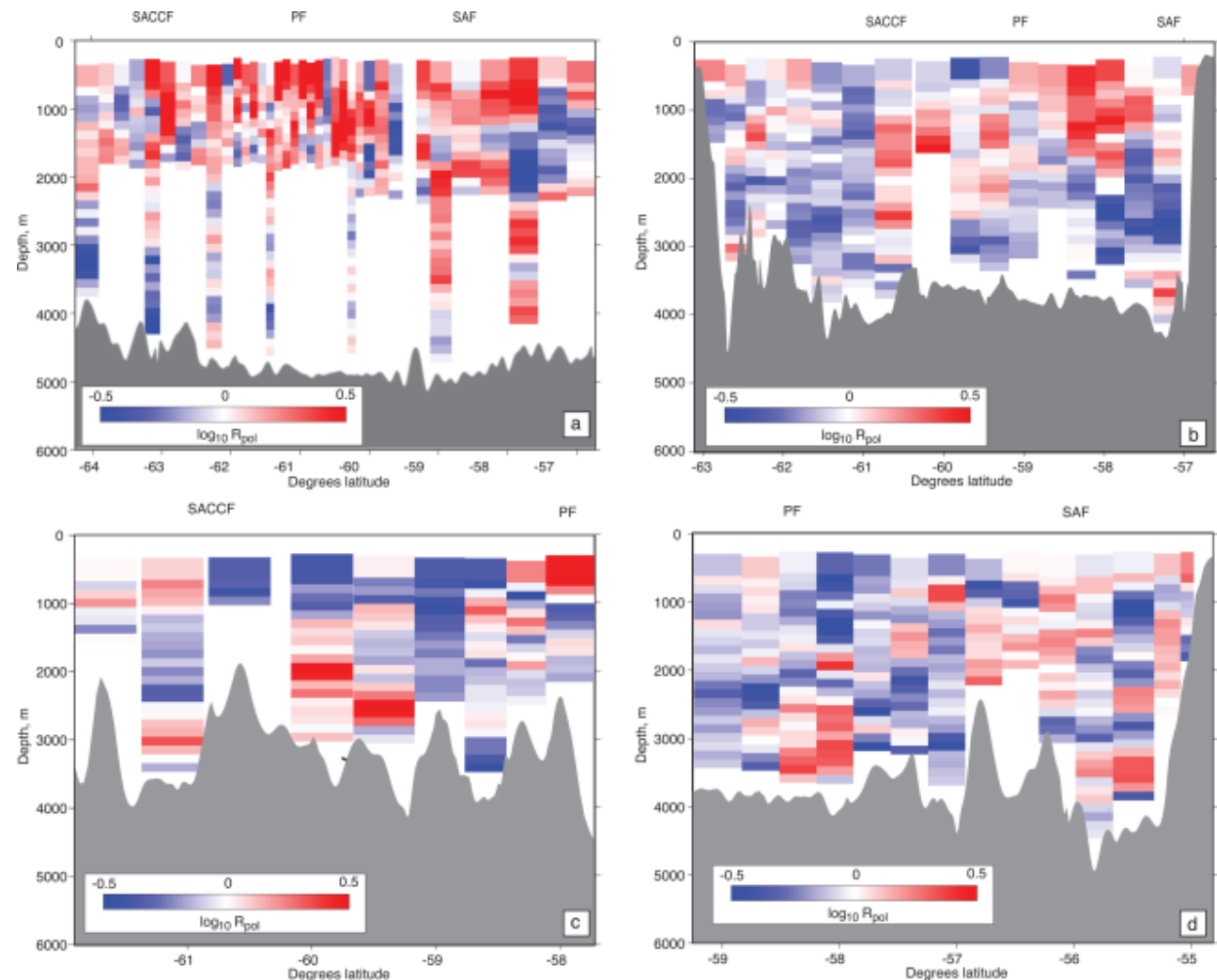
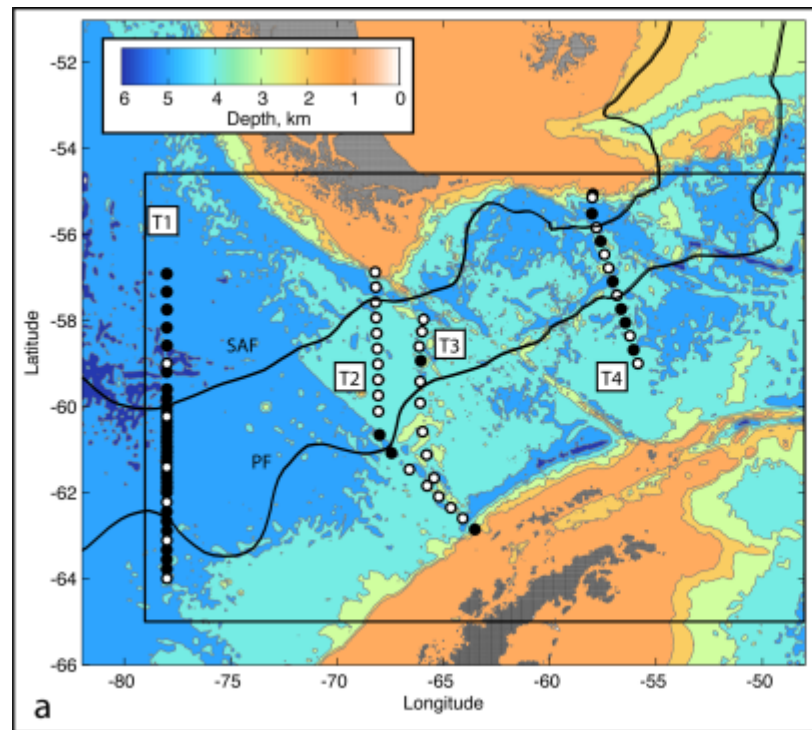


Fig. 4. Clockwise (CW) and anticlockwise (ACW) vertical wave number spectra obtained by averaging the vector spectra of nine profiles in the time series. At high vertical wave numbers the slope of the total spectrum (the sum of ACW and CW spectra above) is approximately -2.5 on the log-log plot. This slope decreases at lower vertical wave numbers. The unit NCM/S is 'normalized centimeters per second,' and SDB is 'stretched decibars.' The normalization and stretching are described in the text.

Leaman and Sanford, JGR 1975

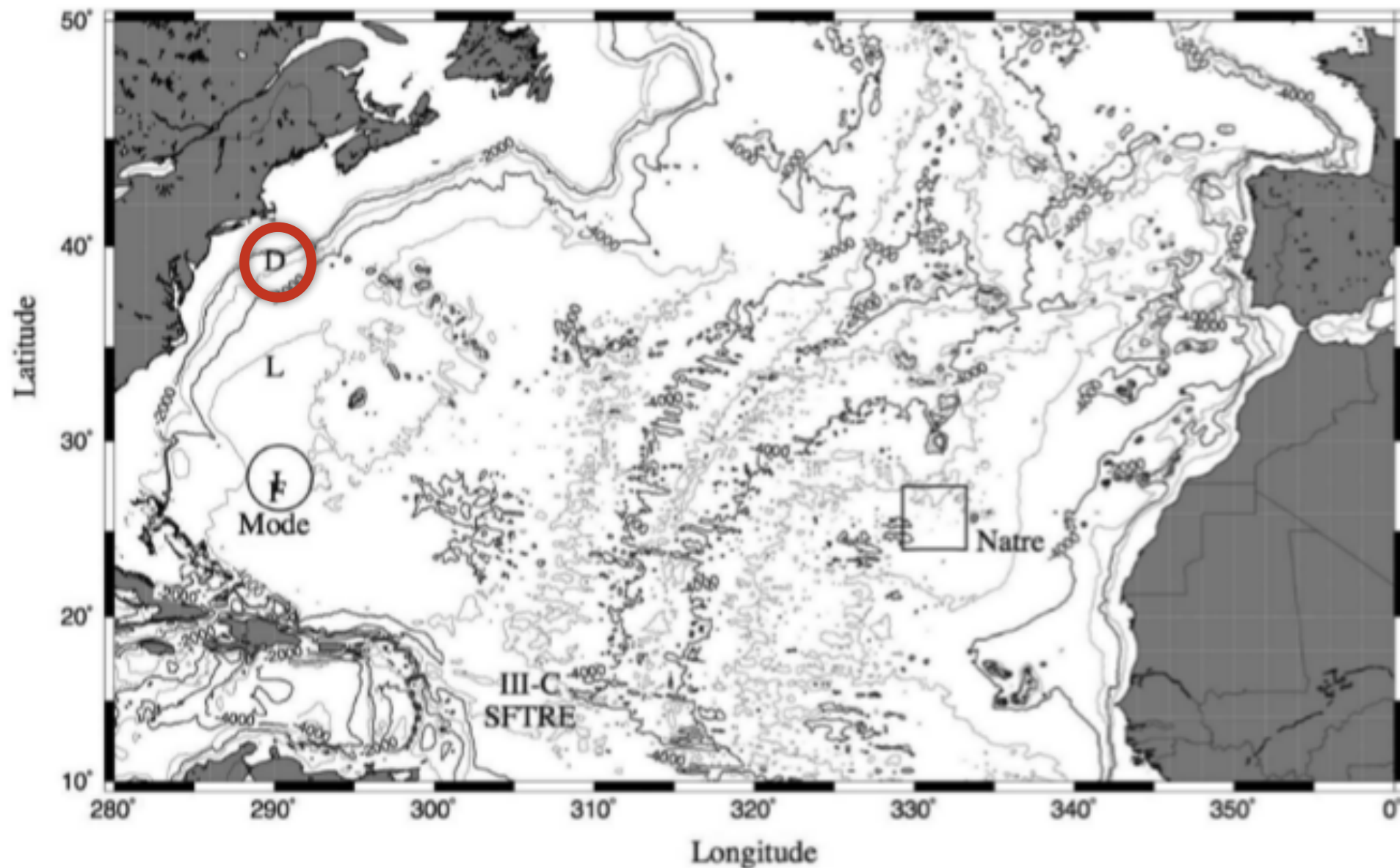
Rotary spectra



Vertical distribution of the polarization ratio across transects T1, T2, T3, and T4, respectively. R_{pol} is computed by integrating counterclockwise and clockwise shear spectra from LADCP measurements. $R_{pol} > 1$ indicates a dominance of downward propagating internal wave energy.

Sheen et al. JGR 2014

Garrett-Munk spectrum



Polzin and Lvov, Review of Geophysics, 2011

Garrett-Munk spectrum

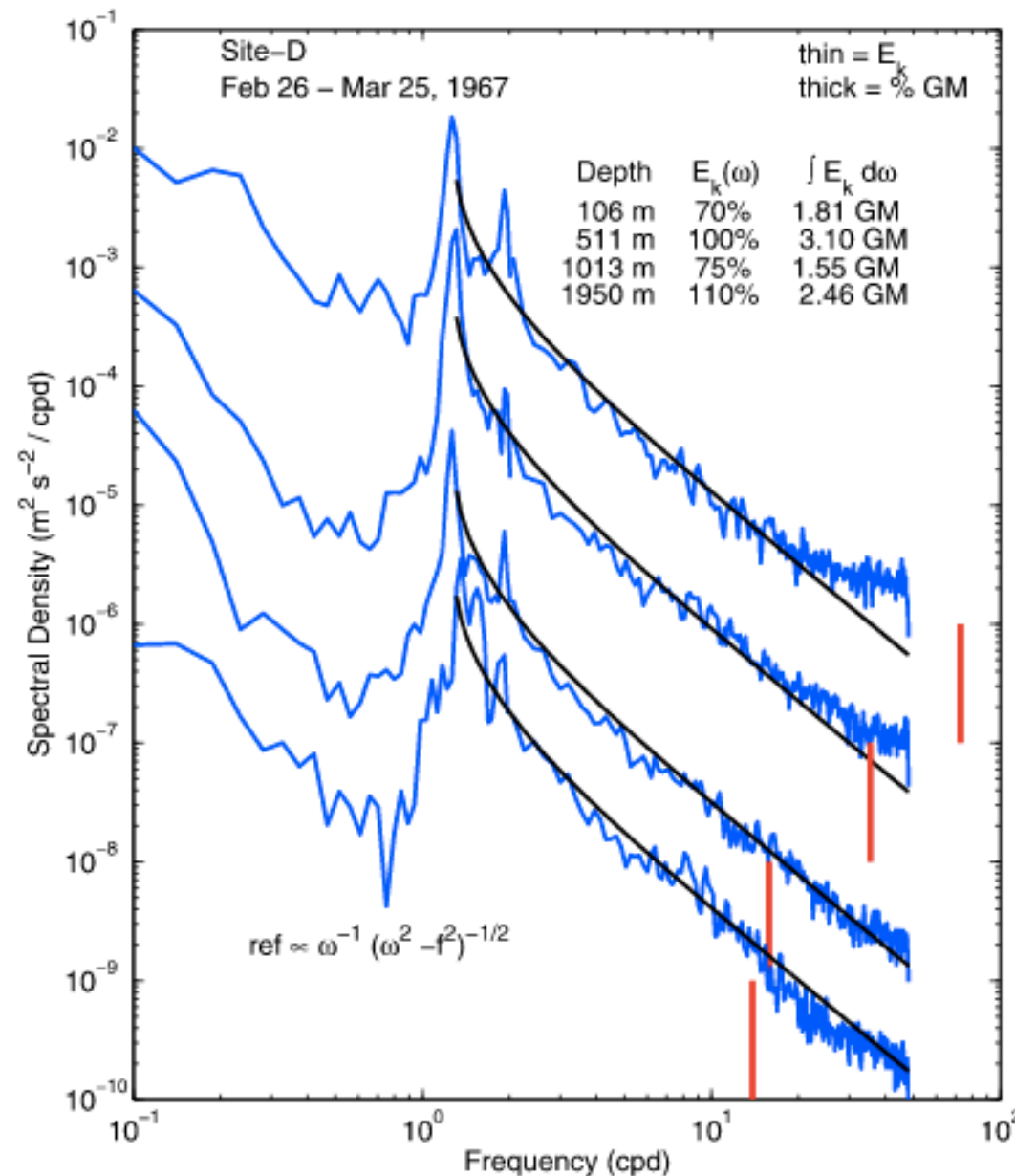
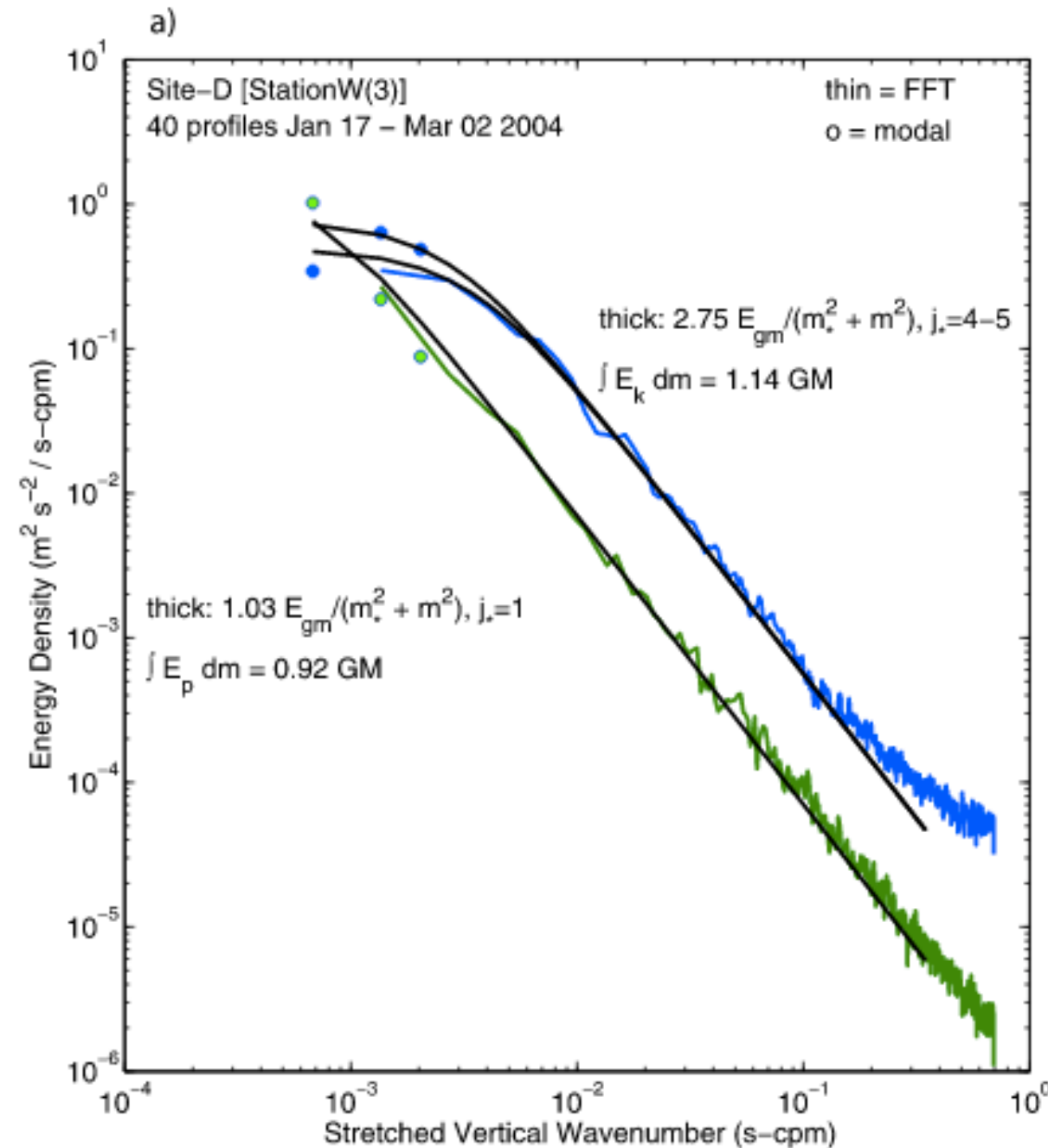


Figure 2. Site D frequency spectra of horizontal kinetic energy (blue lines). These are the Site D data that appeared in the original GM72 paper. Black curves represent fits of (21) with $r = 2$. The thick vertical lines represent the buoyancy frequency cutoff. The spectra have been offset by 1 decade for clarity.

Garrett-Munk spectrum



Polzin and Lvov, Review of Geophysics, 2011

Garrett-Munk spectrum

1. Top and bottom boundaries appear irrelevant in observations made more than about 100m from those boundaries, as though the ocean extended to infinity in both directions
2. The energy levels of internal waves when divided by $N(z)$ are constant within a factor of about 2. When so normalized the RMS motion, as measured either in velocity or vertical displacement, is almost universal in shape both in space and time
3. As much energy is transmitted upward as downward
4. The horizontal transmission of energy is isotropic
5. Two internal wave records, be they temperature or velocity variations, show no visible similarity if they are separated in the horizontal by more than about a kilometer or in the vertical by about 100 m

$$\Phi_E(\omega, m_n) \equiv b^2 N_0 N(z) E(\omega, m_n)$$

$$E(\omega, m_n) \equiv \frac{2}{\pi} \frac{f}{\omega} \frac{6.3 \times 10^{-5}}{(\omega^2 - f^2)^{1/2}} \left[\frac{(n^2 + 3^2)^{-1}}{\sum_n (n^2 + 3^2)^{-1}} \right]$$

Wunsch, Modern Observational PO, 2015

Garrett-Munk spectrum

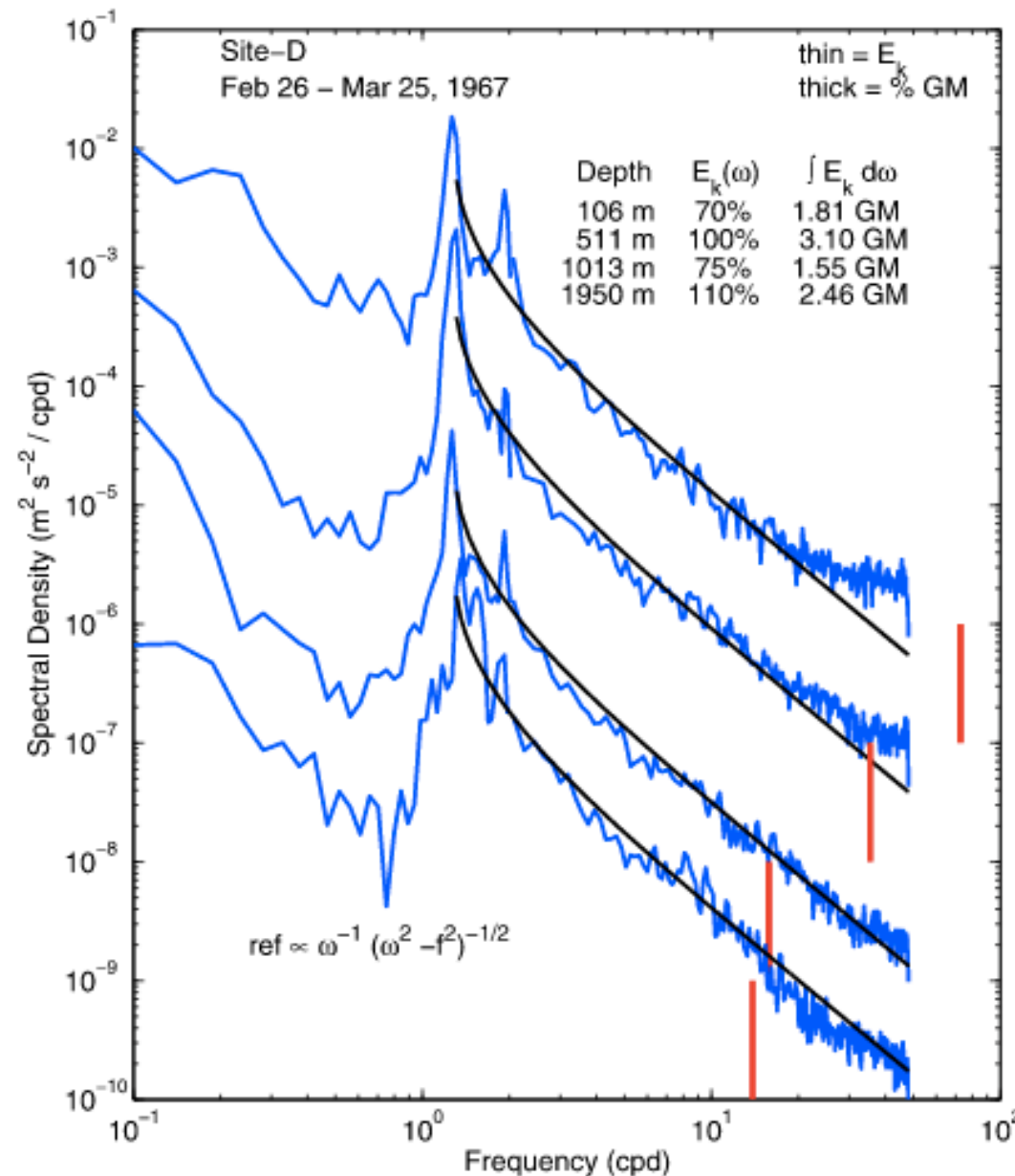


Figure 2. Site D frequency spectra of horizontal kinetic energy (blue lines). These are the Site D data that appeared in the original GM72 paper. Black curves represent fits of (21) with $r = 2$. The thick vertical lines represent the buoyancy frequency cutoff. The spectra have been offset by 1 decade for clarity.

Garrett-Munk spectrum

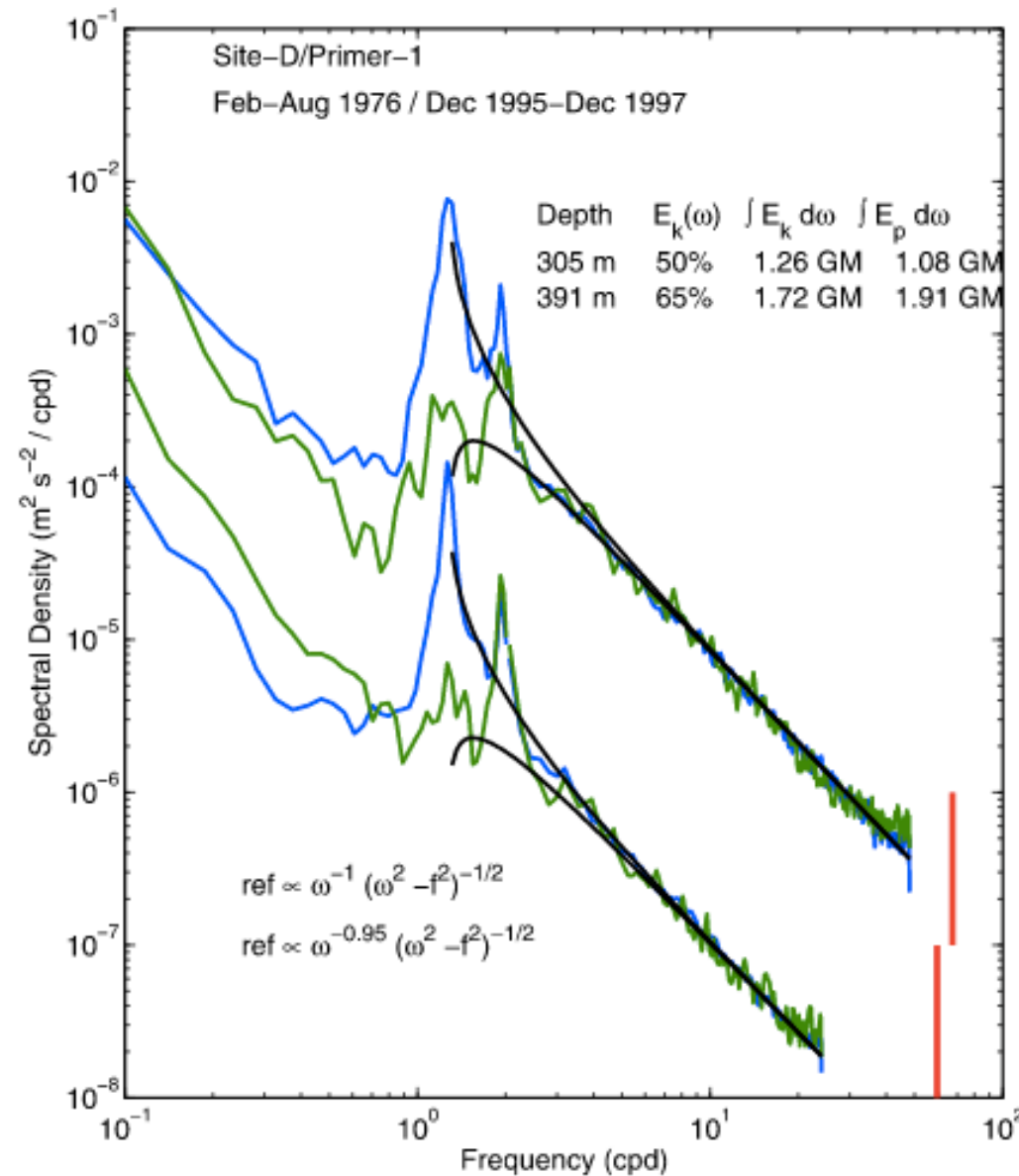
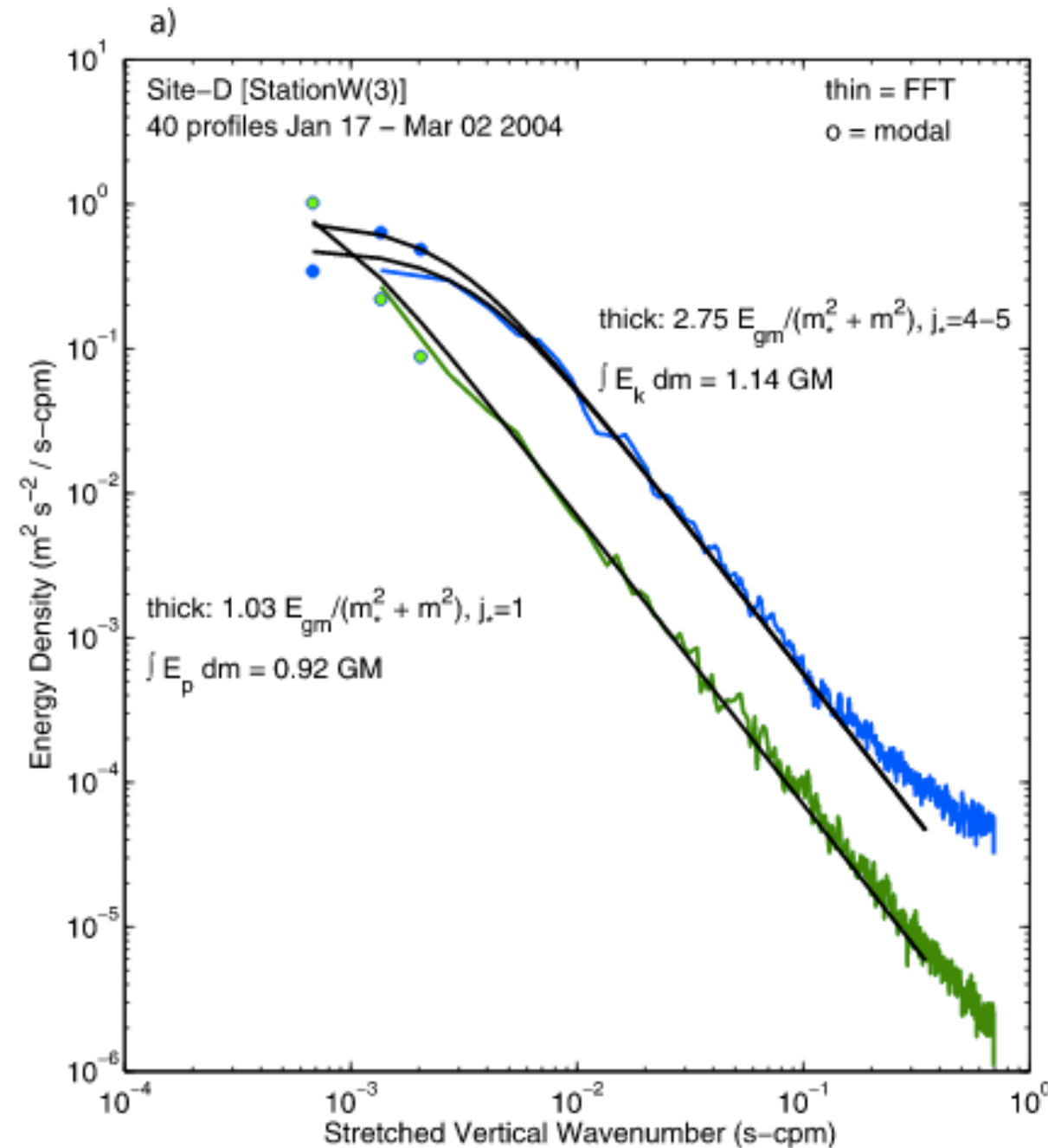


Figure 3. Frequency spectra of horizontal kinetic energy and potential energy (blue and green lines) from nearby Site D. Black curves represent fits of (21) with $r = 2$ and $r = 1.95$. Thick vertical lines represent the buoyancy frequency cutoff. The shape of the fit is stable throughout the 3 decades separating the data in the original GM72 work. Note that the spectral amplitude is somewhat lower than the GM model. The Primer-1 spectra have been offset by 1 decade for clarity.

Garrett-Munk spectrum



Polzin and Lvov, Review of Geophysics, 2011

Garrett-Munk spectrum

$$\Phi_{\zeta}(\omega, m_n) \equiv b^2 \frac{N_0}{N(z)} \frac{\omega^2 - f^2}{\omega^2} E(\omega, m_n), \quad \langle \zeta^2 \rangle = \int d\omega \sum_n \Phi(\omega, m_n)$$

$$\Phi_{KE}(\omega, m_n) \equiv b^2 N_0 N(z) \frac{\omega^2 + f^2}{\omega^2} E(\omega, m_n), \quad \langle u^2 + v^2 \rangle = \int d\omega \sum_n \Phi_{KE}(\omega, m_n)$$

$$E(\omega, m_n) \equiv \frac{2}{\pi} \frac{f}{\omega} \frac{6.3 \times 10^{-5}}{(\omega^2 - f^2)^{1/2}} \left[\frac{(n^2 + 3^2)^{-1}}{\sum_n (n^2 + 3^2)^{-1}} \right]$$

Polzin and Lvov, Review of Geophysics, 2011